Available online at www.sciencedirect.com
ScienceDirect
Bioorganic & Medicinal Chemistry 16 (2008) 1309–1318
Bioorganic & Medicinal Chemistry

Binding effect and design of a competitive inhibitory peptide for HMG-CoA reductase through modeling of an active peptide backbone

Valeriy Viktorovich Pak,[a,*] Minseon Koo,[a] Min Jung Kim,[a] Lyubov Yun[b] and Dae Young Kwon[a]

[a]*Food Fusion and Complex Research Division, Korea Food Research Institute, Baekhyon-dong, Poondang, Songnam, Kyongki-do 463-746, Republic of Korea*
[b]*Department of Organic Synthesis, Institute of the Chemistry of Plant Substances, Building 77, Acad. Kh. Abdullaev Street, 700170 Tashkent, Uzbekistan*

Received 24 September 2007; revised 17 October 2007; accepted 18 October 2007
Available online 23 October 2007

Abstract—This study presents an application of two approaches in the design of constrained and unconstrained peptides in an investigation of the peptide binding effect for HMG-CoA reductase (HMGR). In previous works, hypocholesterolemic peptides isolated from soybean were determined as competitive inhibitory peptides for HMGR. Based on the modeling of an active peptide backbone in the active site of HMGR, two peptide libraries for constrained and unconstrained peptides were designed using different amino acids varying in hydrophobicity and electronic properties. Active peptides were selected by the design parameter 'V' or 'Pr', which reflects the probability of active peptide conformations for constrained and unconstrained peptides, respectively. Using peptides designed as mimics of HMGR substrates, and a combination of in vitro test and circular dichroism study, it was found that: (1) peptide binding causes an ordering of secondary structure, reflecting an increase of α-helical content; (2) HMGR binds the peptide without closure of the active site; and (3) peptide binding induces the protein aggregation. The GFPDGG peptide (IC_{50} = 1.5 μM), designed on the basis of the rigid peptide backbone, increases the inhibitory potency more than 300 times compared to the first isolated LPYP peptide (IC_{50} = 484 μM) from soybean. The obtained data imply the possibility of designing a highly potent inhibitory peptide for HMGR and confirm that changes of the secondary structure in the enzyme play an important role in the mechanism of HMGR inhibition.
© 2007 Elsevier Ltd. All rights reserved.

1. Introduction

3-Hydroxy-3-methylglutaryl coenzyme A reductase (HMGR) converts HMG-CoA to mevalonate, with this catalysis constituting a committed step in the biosynthesis of cholesterol. Activity of this enzyme is important to the control of cholesterol levels. Elevated cholesterol level is a primary risk factor of hypercholesterolemia and is associated with diseases such as coronary artery disease, stroke, and peripheral vascular disease.[1,2]

It is known that people of Asian countries have a notably low risk of atherosclerosis due to their high intake of various soy proteins and soy-based foods.[3,4] Food-derived hypocholesterolemic peptides have been isolated from enzymatic digestion of food proteins, including casein, rice, buckwheat, and soybean protein.[5–8]

In previous studies, two hypocholesterolemic peptides (LPYP and IAVPGEVA) were found by analyses of a digested soy glycinin using trypsin and pepsin, respectively.[9,10] Based on an alignment of the amino acid sequence of soy 11S-globulin with the sequence isolated by pepsin, the derivatives of IAVPGEVA and IAVPTGVA peptides were selected and synthesized.[11] Kinetic experiments support that these peptides are competitive inhibitors of HMGR, acting as a bisubstrate.[12] A structure–functional analysis and the activities of the alanine mutants of these peptides suggest that the P-residue is a recognized residue for the nicotinamide component of the NADPH binding site, and that the residues of T

Keywords: Peptides; Inhibitors; Enzymes; Inhibition mechanism; Active conformation.
* Corresponding author. Tel.: +82 31 7089123; fax: +82 31 7099876; e-mail: pakvaleriy@yahoo.com

0968-0896/$ - see front matter © 2007 Elsevier Ltd. All rights reserved.
doi:10.1016/j.bmc.2007.10.064

and E can be seen as mimics of an HMG-moiety for the HMG-CoA binding site.[11,13] A conformational analysis revealed that a 'turn' structure, which includes the P-residue as a conformational constraint in the recognized motif, is a bioactive conformation for peptides, acting like a bisubstrate.[14]

A structural analysis of the catalytic mechanism based on the crystal structure of human HMGR complexed with the substrates revealed that the binding of NADPH causes a conformational change in the C-terminus of the enzyme, resulting in complete closure of the active site.[15] Under consideration of this mechanism, it was proposed that inhibition of HMGR by a competitive inhibitory peptide is associated with conformational changes in the secondary structure of the enzyme–peptide complex, which can be observed in solution using a circular dichroism (CD) technique.

In related works, the microsomal HMGR from rat liver and the catalytic domain of human HMGR (52 kDa) exhibited a reversible cold lability.[16,17] Due to a very high sequence homology between the catalytic portion of Syrian hamster and human HMGR, a similar phenomenon could be expected for the catalytic portion of Syrian hamster HMGR of 52 kDa used in our experiments.[18] To differentiate possible changes in the secondary structure of the enzyme–peptide complex related to cold lability from those of peptide affinity, temperatures of 20 and 37 °C were used in accordance with the beginning (19 °C) and optimal temperatures (37 °C) of enzyme reactivation, respectively.[16,17]

A two-stage approach was applied in the peptide library design. The first was the modeling of the peptide backbone of a competitive inhibitory peptide in the active site of HMGR using previously designed peptides. IAVP and the peptides IAVE, YAVE, IVAE, and YVAE as competitive inhibitors of NADPH and HMG-CoA, respectively, were selected by the design approach for unconstrained peptides.[13] GLPTGG and GFPTGG, acting as a bisubstrate-mimic, were chosen among designed peptides, having the most constrained structures.[14] The second stage was the design of new peptide libraries in order to evaluate the effects of the functional residue on peptide affinity. The binding effect of the selected peptides was then assessed through the use of an in vitro test and circular dichroism (CD) study.

2. Results

2.1. Modeling of the peptide backbone in active site

The spatial arrangement of model structures of peptides in active site was assessed on the basis of bioactive conformation of statins extracted from the crystal structure of HMGR–statin complexes deposited in the Protein Data Bank: (PDB codes: 1HW8 (compactin), 1HW9 (simvastatin), 1HWI (fluvastatin), 1HWJ (cerivastatin), 1HWK (atorvastatin), and 1HWL (rosuvastatin)). The root mean square distance (RMSD) was applied to compare locations in the active site at either the peptide backbone or the side chain of peptides (I-, L-, F-, and Y-side chains in accordance with *iso*-butyl or 4-fluorophenyl radicals of statins). All peptide models were grouped according to the (1) peptide backbone and (2) location of the side chain. The first group includes the IAVE, YAVE, IVAE, and YVAE peptides. On the basis of consideration of the *iso*-butyl radical and benzene ring, IAVE, IVAE, and GLPTGG and YAVE, YVAE, and GFPTGG comprise the second and third groups, respectively. As a common binding point for statin and peptide molecules, the mimic of HMG-moiety in statin and peptide structures was fixed at the same location for all groups.

For the first group, which comprises unconstrained peptides, the model structure for IAVE, YAVE, IVAE, and YVAE peptides was built on the basis of an 'active space' constructed by the superposition of bioactive conformation of statin molecules, as was described in a previous work (Fig. 1a).[13] Based on the differentiation of the 'active space' and the determined probabilities of a peptide population in each interval, the model structure was calculated as the average structure using the peptide population with the highest value of probability.[13] By considering the highest peptide activity in the first group, the model structure of the YVAE backbone was used as a basis for comparison. To assess the model structures, the dependence of $\log(IC_{50})$ from the RMSD values of the peptide backbone was plotted (data not shown). The obtained correlation coefficient (r^2) of 0.97 indicates a strong correlation between the peptide activity and the calculated structure of the peptide backbone. This finding indicates that the model structure determined for each peptide can be used for a comparative investigation involving the location of the side chain for peptides of the second and third groups.

Location of the side chain of peptides was compared to that of *iso*-butyl (compactin and simvastatin) and the benzene ring of the 4-fluorophenyl radical of statins (fluvastatin, cerivastatin, atorvastatin, and rosuvastatin). In a previous work, the constrained GLPTGG and GFPTGG peptides were designed according to the most rigid peptide backbone.[14] Based on the CD spectra in the TFE/water mixture, type II of the β-turn was considered as a major structural element in these peptides.[14] The model structures were built up as type II of the β-turn on the basis of the backbone dihedral angles adopted by the two corner residues P and T ($\varphi_{i+1} = -60°$, $\psi_{i+1} = 120°$, $\varphi_{i+2} = 80°$, and $\psi_{i+2} = 0°$) (Fig. 1b). The peptide conformations were defined by the arrangement of the head (H) and tail (T) of the peptide relative to the β-turn on the basis of the plane passing through the three α-carbon atoms of 2, 3, and 5 from the N-terminus. The minimized energy conformations were used as starting structures in a molecular dynamics (MD) simulation. By considering the smallest standard deviation of the torsion angle determined for the peptide backbone and a combination of the α-carbon atoms with the carbon atoms of the side chains, the most restricted peptide structure was determined for the (-H:-T) conformation.

Figure 2 shows that the location of the geometric centers of the benzene ring of peptide molecules is close to that

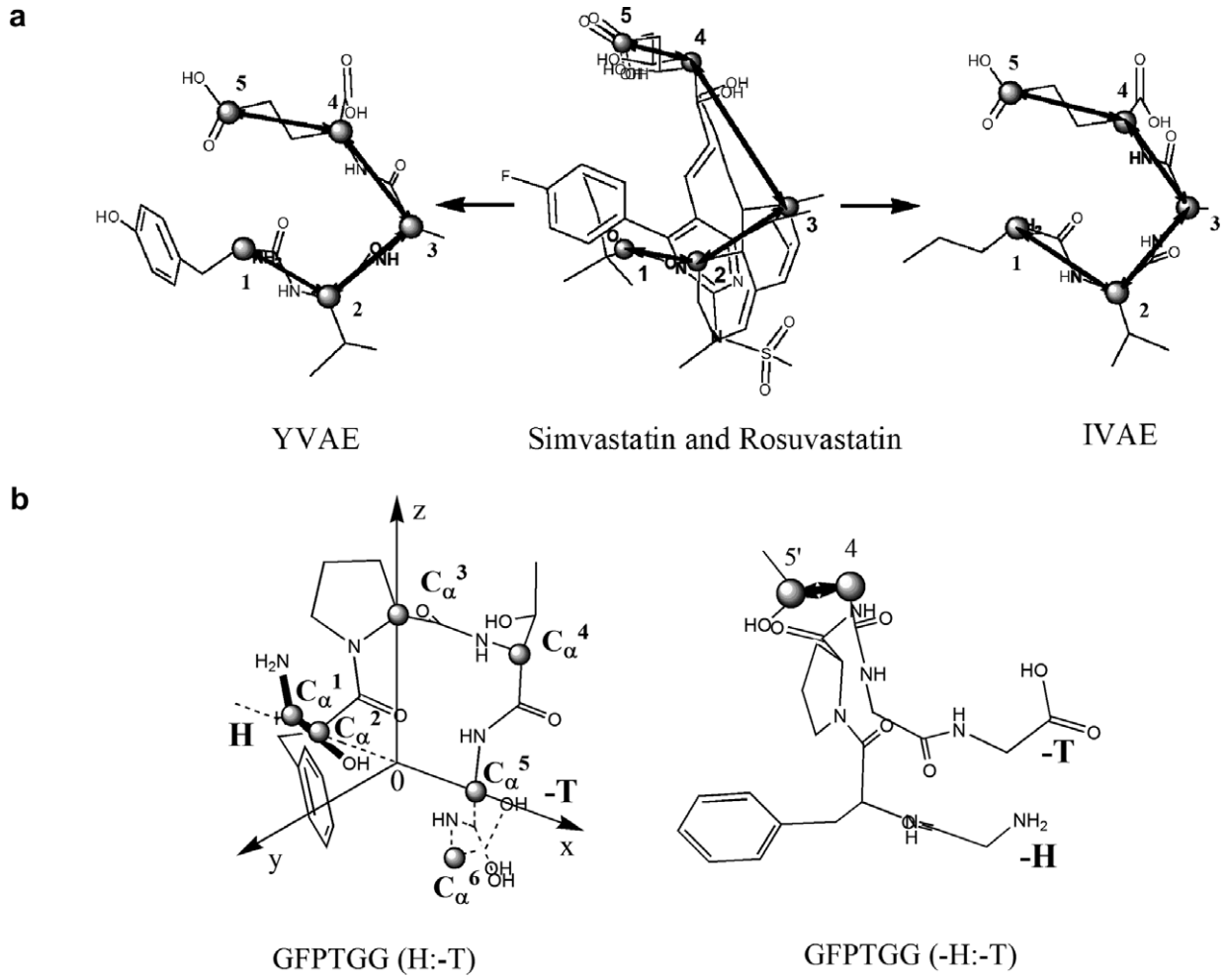

Figure 1. Models of HMG-CoA competitive inhibitory peptides (a) and peptide acting as a bisubstrate (b). (a) Model of an 'active space' (tetrahedron 1-2-3-4) based on a superposition of the bioactive conformations of simvastatin and rosuvastatin extracted from the crystal structure of HMGR–statin complex (PDB codes: 1HW9 (simvastatin), 1DQA (rosuvastatin)), and the average structures determined for IVAE and YVAE peptides. (b) Model of the type II β-turn in peptide conformer (-H:-T) with an arrangement of peptide head ((H)-bold) and tail ((T)-short-dashed) relative to the plane passing through the three α-carbon of 2, 3, and 5 atoms of the peptide backbone, and the peptide conformation (-H:-T) used in this study. The 4–5 and 4–5′ fragments in the peptide models were fixed as an HMG-mimic during modeling.

of statin molecules with a RMSD value of 0.03 Å between the statin and peptide centers. For *iso*-butyl radical, the same location of bioactive conformations of compactin and simvastatin in the active site was found, and the difference between the statin and peptide centers was determined to be 0.51 Å. The consistency of these results suggests similarity in the location of the I-, L-, F-, and Y-side chains of peptides in the active site of HMGR.

2.2. Peptide library design

Analyses of statin and peptide structures in the active site of HMGR led to the proposition that the location of the I-, L-, F-, and Y-side chains of peptides plays an important role in the peptide activity. To better define the nature of the peptide–protein interaction of these residues in terms of hydrophobicity, electronic properties, and active peptide conformation, six new peptides were assessed by the design approach for unconstrained peptides. Based on IAVE, YAVE, IVAE, and YVAE as unconstrained peptides, the N-terminus residues were replaced with two amino acids: phenylalanine and tryptophane. Thus, we changed hydrophobic side chains of original residues (*iso*-butyl and 4-hydroxyphenyl). To assess electronic properties of aromatic moieties, the hydroxyl group of Y residue was substituted by a halogen atom in position 3 or 4 (fluorophenylalanine and chlorohenylalanine). Based on these consideration, the peptides FVAE, WVAE, F(4-Fluoro)VAE, F(4-Chloro)VAE, F(3-Fluoro)VAE, and F(3-Chloro)VAE were chosen as candidate peptides for the peptide library. Further, conformations of the selected peptides were assessed by the design criterion 'Pr', reflecting the probability of active peptide conformations.[13]

In order to better define the interactions in HMG-binding site, the designed rigid backbone of the constrained GFPTGG and GLPTGG peptides was used as a basis for GFPDGG, GFPEGG, GLPDGG, and GLPEGG peptides. IAVPGEVA was added as a control compound for this peptide library. Constrained peptides

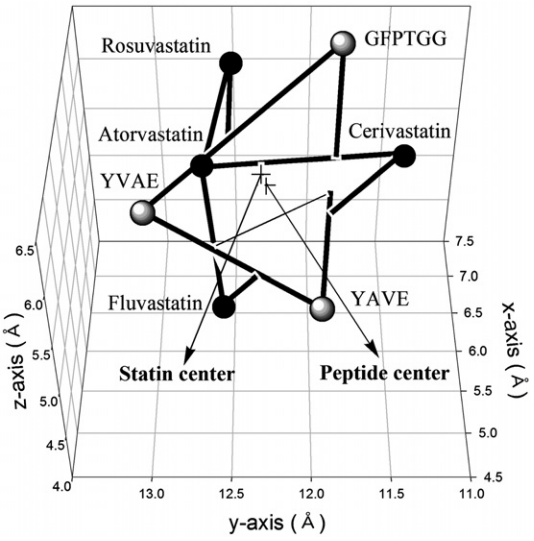

Figure 2. A 3D view of the location of the geometric center of the benzene ring of the 4-fluorophenyl radical for statins (●) and the 4-hydroxyphenyl and phenyl radicals for peptides (●) based on the Cartesian coordinates of the model structures. Location of the average geometric centers of the statin and peptide models is shown as the 'statin center' and 'peptide center'.

were assessed by the design criterion 'V', which reflects a rigidity of the peptide backbone.[14]

The results of the design criteria for unconstrained (Pr) and constrained (V) peptides are shown in Figure 3. According to the 'Pr' value, FVAE and F(4-Fluoro)VAE have relatively higher values compared with WVAE and halogen-contained peptides, respectively (Fig. 3a). By considering the 'V' parameter, the GFPDGG and GFPEGG sequences are the most rigid structures compared to the other peptides (Fig. 3b). Thus, these peptides were synthesized to assess a role of the selected residues in the peptide affinity. GVAE and GGPTGG peptides were additionally synthesized to provide a negative control of the I-, L-, F-, and Y-side chain contributions in the peptide activities.

2.3. Assessment of inhibitory activity of the synthetic peptides

Each of the synthesized peptides showed an ability to inhibit HMGR, with the exception of the GVAE and GGPTGG peptides (Table 1). The activities of the GVAE and GGPTGG peptides were not detectable, even at high concentrations. This indicates that the location of the I- and L- and F- and Y-side chains plays an important role in the peptide–protein interaction in the active site of HMGR. For FVAE, our results indicated that increase of the hydrophobic character led to peptide showing a lower activity compared to YVAE. Location of a fluorine atom in position 4 on the F residue led to significant improvement of affinity. Increase of the inhibitory activity (IC_{50}) was also found for GFPDGG (1.5 μM) and GFPEGG (1.7 μM) compared to GFPTGG (16.9 μM).

To estimate the peptide backbones, the dependences between observed and predicted peptide potency were

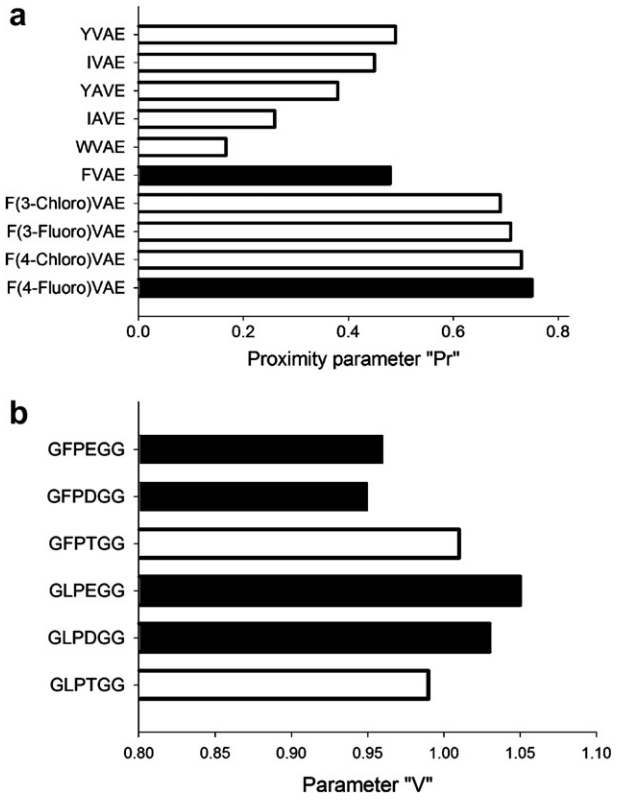

Figure 3. Calculated 'Pr' (unconstrained structure (a)) and 'V' (constrained structure (b)) parameters for each member of the peptide library. Peptides, marked in black, were selected as active compounds.

plotted for unconstrained and constrained peptides. Figure 4 shows good correlations between the experimental activity of the peptides, measured by $\log(IC_{50})$, and the predicted activity obtained through the 'Pr' ($r^2 = 0.98$) and 'V' ($r^2 = 0.96$) parameters. This finding suggests that the peptide backbones of the designed sequences are close to the active peptide conformations.

In order to assess the positional relationship of peptides in the active site, competitive inhibitory peptides of NADPH, HMG-CoA, and both substrates were tested in different combinations. From in vitro assays of the susceptibility of HMGR to inhibition by given peptides, we found synergy in the ability to inhibit HMGR when IAVP was combined with IAVE, YAVE, IVAE, and YVAE (Table 2). As expected in accordance with the arrangement of peptides in the active site, the synergistic properties were not observed for combinations of IAVP or HMG-CoA-mimic peptides with the bisubstrate-mimic peptide (GLPTGG, GFPTGG, GFPDGG, and GFPEGG).

Based on the obtained data for tested combinations at a peptide ratio of 1:1, the dependency between relative inhibitory activity and peptide sequence was plotted. Figure 5a shows that in combinations, the inhibitory activity of IAVP and peptides acting as competitive inhibitors of HMG-CoA was increased 7- and 3-fold, respectively. This leads to the proposition that structural changes to the NADPH binding site interplay with occupation of the HMG-CoA binding site by a peptide.

Table 1. Summary of the sequence structures and inhibitory activities (IC_{50}) of the isolated and designed peptides used in this study

Peptide sequence	Peptide description	IC_{50} (μM)
LPYP	Peptide isolated from soybean by trypsin	484.7
IAVPGEVA	Peptide isolated from soybean by pepsin	152.1
Unconstrained peptide		
IAVP	NADPH competitive inhibitor	97.1
IAVE	HMG-CoA competitive inhibitor	75.2
YAVE	HMG-CoA competitive inhibitor	52.6
IVAE	HMG-CoA competitive inhibitor	44.1
YVAE	HMG-CoA competitive inhibitor	41.8
FVAE	HMG-CoA competitive inhibitor	43.8
F(4-Fluoro)VAE	HMG-CoA competitive inhibitor	3.8
GVAE	Negative control (I- and Y-side chains)	Inactive
Constrained peptide		
GLPTGG	NADPH and HMG-CoA competitive inhibitor	19.4
GLPDGG	NADPH and HMG-CoA competitive inhibitor	22.3
GLPEGG	NADPH and HMG-CoA competitive inhibitor	27.2
GFPTGG	NADPH and HMG-CoA competitive inhibitor	16.9
GFPDGG	NADPH and HMG-CoA competitive inhibitor	1.5
GFPEGG	NADPH and HMG-CoA competitive inhibitor	1.7
GGPTGG	Negative control (L- and F-side chains)	Inactive

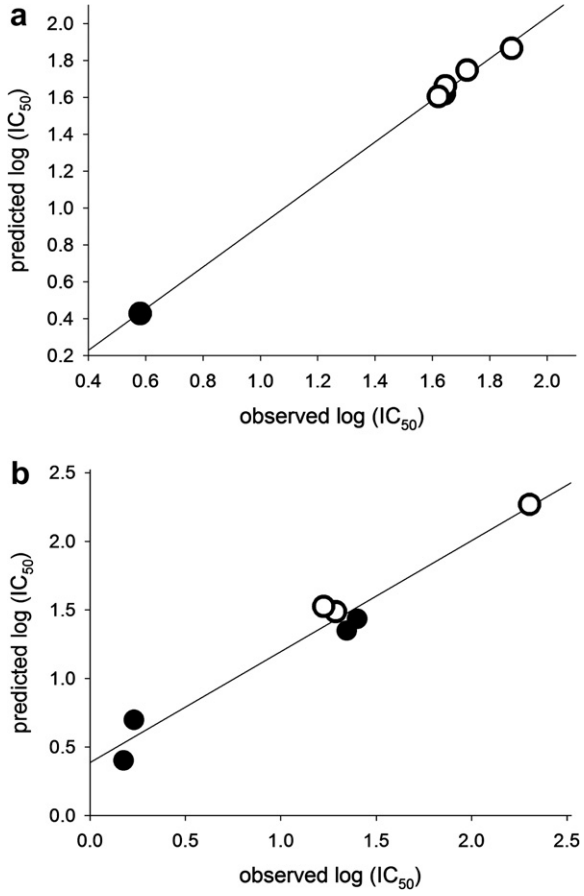

Figure 4. Correlation between observed peptide potency and predicted potency against HMGR for designed peptides and initial peptides with unconstrained (a) and constrained (b) structures measured by in vitro assay. The correlation coefficients, r^2, are 0.98 (a) and 0.96 (b). The designed peptides (●); initial peptides (○).

For IAVP and YVAE peptides, two additional peptide ratios were tested (Table 2). The turning points observed in the relative changes in inhibitory activity of IAVP and YVAE indicate the best ratio for these peptides among tested combinations (Fig. 5b). An increase in inhibitory activity from 5- to 10-fold for IAVP and from 2- to 5-fold for YVAE suggests that HMGR binds IAVP and YVAE without steric hindrance between these peptides in the active site.

Table 2. Inhibitory activity of IAVP in combination with peptides designed as a competitive inhibitor of HMG-CoA

No.	Combination	EC_{50}[b] (μM)	CI[a] at the following percent inhibition	
			75	90
1	IAVP + IAVE (1:1)	125.62	0.85	0.66
2	IAVP + YAVE (1:1)	80.54	0.45	0.36
3	IAVP + IVAE (1:1)	52.06	0.34	0.27
4	IAVP + YVAE (1:1)	30.06	0.19	0.14
5	IAVP + YVAE (1:2)	29.94	0.13	0.11
6	IAVP + YVAE (2:1)	29.40	0.28	0.21

[a] The table shows the CIs for 75% and 90% inhibition of HMG-CoA reductase and EC_{50} for combinations. The CI value compares the amount of drug A which gives 75% or 90% effect when used in combination with another drug B, with the amount of drug A which gives 75% or 90% effect when the drug is used alone. A combination is either synergistic, additive, or antagonistic if CI <1, =1, >1, respectively.[19] The values were determined from three independent experiments.

[b] The EC_{50} for the combination is the concentration of IAVP added to the concentration of another peptide at which 50% inhibition was achieved.

2.4. Circular dichroism study of the HMGR–peptide complex

In order to investigate the conformational behavior of the peptide-bound complex, we first assessed a combination of IAVP and YVAE peptides at low peptide concentrations under a temperature approximating that of the beginning of enzyme reactivation (19 °C). Figure 6a presents the spectra of HMGR complexed with peptides as a function of the peptide concentration at 20 °C.

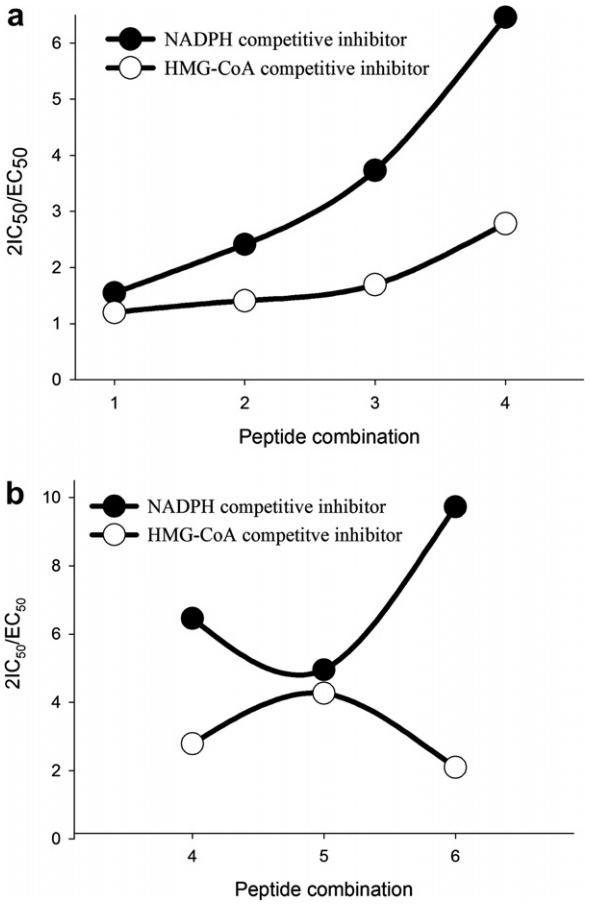

Figure 5. The relative changes in inhibitory activity of peptides in combination (EC_{50}) compared to the individual used (IC_{50}) for a peptide ratio of 1:1 (a) and for a mixture of IAVP and YVAE at different ratios (a). Mean peptide activity change in tested combinations was calculated on the basis of Table 2.

At this temperature, as the concentration of peptides under an IAVP:YVAE ratio of 1:1 rises from 6.25 to 25.0 μM, ellipticity increases as a function of concentration. Notably, the relative increase is greater at 208 and 222 nm than at 218 nm, indicating a concentration-dependent increase in α-helical content. Inspection of CD spectral absorptions obtained at 20 °C revealed that the α-helical content increased when the peptide concentrations were increased from approximately 28.2% for HMGR alone to 36.3% for peptide-bound HMGR, and β-content was retained in a range of 27.7 ± 2.1%. A similar CD absorption profile of HMGR alone was described in study.[20] According to the content of the peptide-bound structures, a major change in the secondary structure of the enzyme–peptide complex with an increase of peptide concentration was found with respect to α-helical content. This finding indicates that the content of α-helical structure might be chosen as a criterion for conformational changes in the enzyme–peptide complex.

Based on the selected criteria, the critical-induced aggregation concentration (C_{CIAC}) for all peptides was determined by the dependence of the α-helical structure of the formed enzyme–peptide complex in a wide range of peptide concentrations (Fig. 6b and c). The resulting curves show that values of C_{CIAC} for peptide combinations and bisubstrate-mimic peptides lie in 50–75 and 12–25 μM concentration intervals, respectively. Based on the insignificant alterations in α-helical content above a peptide concentration of 75 μM in all cases, it was concluded

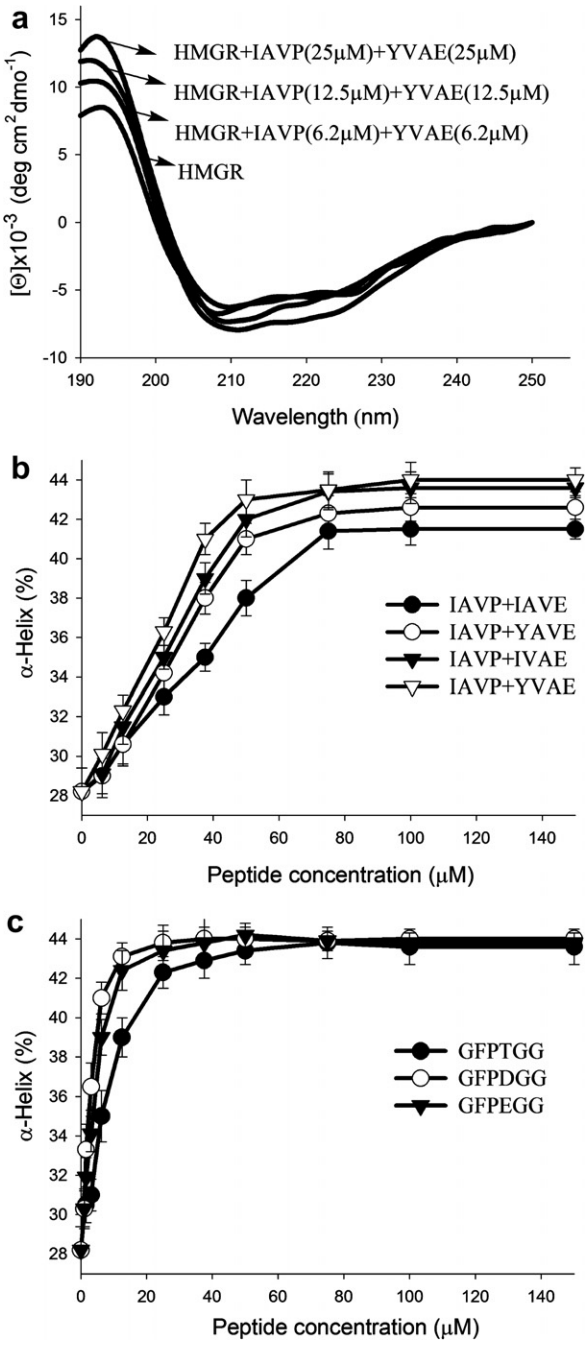

Figure 6. α-Helical structural dependency of HMGR–peptide/s complexes from peptide concentration at 20 °C. (a) CD spectra of HMGR and its complex with IAVP and YVAE under low peptide concentrations (peptide ratio 1:1). (b) For HMGR bound with IAVP and HMG-CoA-mimic peptides. (c) For HMGR bound with bisubstrate-mimic peptides. Mean residue ellipticity [Θ] data at the indicated wavelengths are average values for five scans. Spectra presented in 20 mM K_xPO_4, pH 7.0, under a concentration of 71 μg protein/mL of HMGR using 1 mm pathlength cell. Secondary structure content was determined using a neural net analysis program K2D.

that this concentration could be used in the subsequent comparative investigation of the conformational behavior of HMGR–peptide complex in solution. Using this concentration, the content of the secondary structure of HMGR–peptide complexes at 20 °C was compared with that at 37 °C (data not shown). A minor deviation in the secondary structure content was observed between them. Furthermore, a concentration-dependent change in the secondary structure was not found at 37 °C. For HMGR, the α-helical content was increased up to 37.9%, which was higher than at 20 °C (28.2%), with minor changes in the β-structure.

2.5. Thermal unfolding study of the HMGR–peptide complex

In order to determine the stability and dissociation properties of the formed peptide-bound complexes, a thermal unfolding study was applied. By considering the optimal temperature of 37 °C for enzyme reactivation and the C_{CIAC} values, a temperature interval from 37 to 80 °C and a peptide concentration of 75 μM were selected. The melting curves obtained for peptides are essentially identical to the thermal scanning profile of HMGR alone (Fig. 7). In all cases, the melting curves were nonsigmoidal denaturation curves, reflecting a gradual and incomplete heat denaturation process. The observed differences in slopes of the melting curves are consistent with the peptide-dependent changes in the secondary structures. This finding proposes that α-helical content is stabilized when HMGR binds peptides and induced by peptide binding. Figure 7b shows the difference in stability of the formed enzyme–peptide complex induced by a mixture of IAVP and YVAE peptides compared to that when these peptides are used alone. The slopes of the melting curves for the enzyme bound with either IAVP or YVAE are quite similar, indicating the formed complexes have similar stability. This proposes that each peptide makes respective contribution to change the secondary structure of the formed complex when the enzyme binds the peptide mixture.

2.6. Analysis of the conformation changes in HMGR–peptide complex

Based on the data of the C_{CIAC} values and the confirmed stability of the peptide-bound complexes we analyzed the relationship between the conformational changes in the active site of the HMGR–peptide complex and peptide binding. An assessment of the average secondary structure content for peptide-bound complexes at a peptide concentration of 75 μM yielded values of 43.3% for α-helix and 27.7% for β-sheet. The substrate-bound and statin-bound crystallographic structures deposited in the Protein Data Bank have a similar average secondary structure content determined as 45.5% (α-helix) and 27.3% (β-sheet), and 42.8% (α-helix) and 29.3% (β-sheet), respectively (PDB access codes: 1dqa, 1dq8, 1dq8, 1HW8, 1HW9, 1HWI, 1HWJ, 1HWK, and 1HWL).[15,20] By considering the completed process of aggregation at 37 °C determined for HMGR, the conformational changes in the active site associated with peptide affinity were calculated as the difference between the α-helical content at

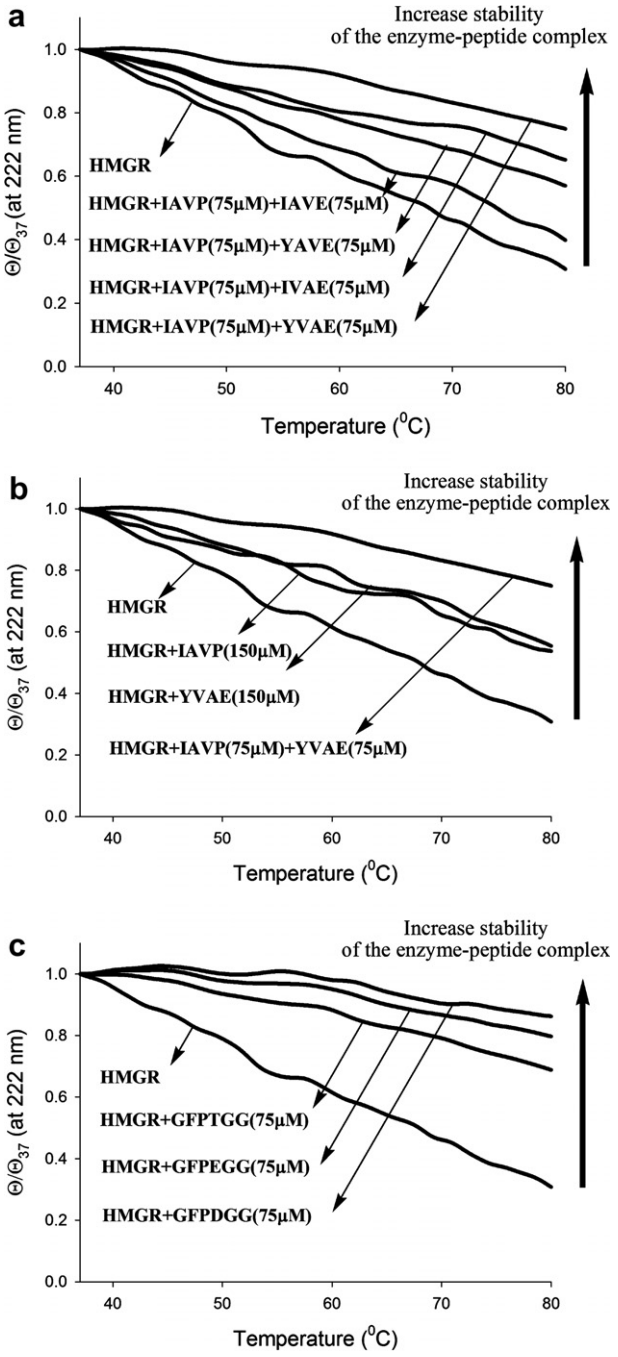

Figure 7. Thermal scanning of CD signal of HMGR and its peptide-bound complex in a temperature range from 37 to 80 °C at 222 nm. The data were normalized relative to the CD signal at 37 °C: (a) for HMGR alone to −8.51, complex HMGR with IAVP and IVAE to −11.49, IAVP and IAVE to −11.03, IAVP and IVAE to −11.26, IAVP and YVAE to −11.53 (mdeg cm^2 dmol^{-1}); (b) complex HMGR with IAVP to −10.64, YVAE to −10.11 (mdeg cm^2 dmol^{-1}); (c) complex HMGR with GFPTGG to −11.09, GFPDGG to −11.62, GFPEGG to −11.47 (mdeg cm^2 dmol^{-1}).

37 °C using peptide concentrations of 75 and 0 μM. Based on the values of IC_{50} and EC_{50} for peptide combinations 1–4, we calculated the increment of peptide activity in combination for IAVP and HMG-CoA-mimic peptides (Table 2). Plotting the dependence of the difference in α-helical content associated with conformational changes

in the active site from the logarithm of the increment of the peptide activity, the linear dependences with the correlation coefficient (r^2) were found to be 0.96 (IAVP) and 0.84 (HMG-CoA-mimic peptides). For GFPTGG, GFPDGG, and GFPEGG, the r^2 of the linear dependence between the changes in the active site induced by these peptides and log(IC_{50}) was determined as 0.87. The consistency of these results indicates that the determined conformational changes in the secondary structure of the enzyme–peptide complex are associated with the peptide affinity in the active site of HMGR.

3. Discussion

The estimated data of the secondary structure of HMGR combined with either a peptide or a combination of peptides provide evidence of the occurrence of conformational changes in the formed complexes. The results of the CD experiment can possibly explain the aggregation process observed by the concentration-dependent changes in the secondary structure of the peptide-bound complex. The dissociation of subunits at low temperature is considered a source of cold lability. The monomer of hamster HMGR includes two dimerization motifs that are highly conserved among I and II classes of HMGR.[15] The first is β-sheet, which is close to the N-terminus, and contributes residues to establish hydrogen bonds between the equivalent amino acids of the neighboring monomer. Another dimerization motif consists of two helixes with a catalytically important D residue between them.[15] It is possible that the peptide initiates conformational changes in the catalytic site associated with ordering of these two helixes of the dimerization motif. The concentration-dependent changes observed in the α-helical structure with minor alteration in the β content also support this model considering the changes in secondary structure.

Synergy observed in the inhibition activity of peptides acting as competitive inhibitors of NADPH and HMG-CoA supports that the actions of peptides are unchanged and HMGR binds peptides at different binding sites. According to the crystallographic analyses of substrate-bound and statin-bound structures, the C-terminal residues of HMGR proteins are a mobile element. In the enzyme–statin structures, the innate flexibility of this region is exploited by the statin molecules to create a binding site for themselves.[21] A similar effect in changes of the C-terminal residues can also be expected in the case of the peptide binding. The higher value of r^2 obtained for IAVP compared to HMG-CoA-mimic peptides also supports this supposition. By considering the equilibrium constant of inhibitor binding (K_i) and the kinetics of the enzyme–peptide complex formation, the difference in synergy observed under different peptide ratios suggests that the conformational change is not associated with complete closure of the active site, as in the case of substrate binding, and the HMGR active site is accessible for peptide molecules.[15]

The difference observed in synergistic properties when YAVE or YVAE is combined with IAVP, as well as in the case of IAVE and IVAE, could be explained by the different effect of the electrostatic interactions appeared at the active site, linking with different orientations of the peptide backbone in the binding pocket. The high value of r^2 (0.97) between log(IC_{50}) and the RMSD values determined for the average peptide structures, when these peptides were used alone, also supports this proposition. By considering the larger changes observed in the inhibitory activity of IAVP peptide compared to peptides acting as a mimic of HMG-CoA, it can be concluded that a tighter binding pocket is formed for the NADPH mimic peptide.

In combinations 1–4 (Fig. 5a), a minor difference determined between statin and peptide centers regarding location of the aromatic radicals compared to that of the alkyl radicals concurs with the larger increase in IAVP inhibitory activity observed for the mixture with either YAVE or YVAE compared to that of IAVE or IVAE peptides.

GFPDGG and GFPEGG show a 10-fold increase in inhibitory activity compared to the GFPTGG peptide. The retention behavior on RP-HPLC, GFPTGG, GFPDGG, and GFPEGG reflects a close structure in the peptide backbone, because their retention times showed a minor difference in values (8.36, 8.12, and 8.16, respectively). Also, the CD spectra of GFPDGG and GFPEGG exhibit a β-turn II structure in 90% TFE in water with a profile close to that of GFPTGG peptide (data not shown). This suggests that enhancement of the electrostatic interactions between the D- and E-side chains and HMG binding pocket compared to the T-side chain is related to an increase in peptide affinity and conformational changes.

According to the arrangement of peptides in the active site, the similarity in location of the I-, L-, F-, and Y-side chains of peptides designed as mono- and bisubstrate-mimics of HMGR with abolishment of inhibitory activities, as in the case of GVAE and GGPTGG peptides, indicates that the alkyl and aromatic radicals play a special role in retaining the bioactive peptide conformation and also influence the occupied space in conformational changes in the protein.

The linear dependence obtained between conformational changes in the secondary structure of enzyme–peptide complex and peptide activity, as well as with the increment of the peptide activity, shows a fairly strong correlation, thus suggesting that the conformational changes induced by peptide binding play an important role in the mechanism of HMGR inhibition.

In summary, this study elucidates the conformational changes in the secondary structure of the peptide–enzyme complex in the inhibition mechanism of HMGR by peptides. Peptide binding induces conformational changes associated with dimerization and peptide affinity. The present experiments show that HMGR binds peptides without closure of its active site. Based on the conformational behavior of the peptide-bound complex and previously obtained results pertaining to peptide design, the

applied design methods point toward the possibility of modeling a highly potent HMGR peptide inhibitor.

The presented design approaches directed toward minimizing the functional residues and modeling of the peptide structure close to the bioactive conformation provide a good opportunity to study the binding properties related to peptide–protein interactions in cases when no a prior spatial information is available.

4. Experimental

4.1. Materials

H-Gly-2-ClTrt resin (substituted at 0.5 mequiv/g), H-Glu(O*t*-Bu)-2-ClTrt resin (substituted at 0.55 mequiv/g), and Fmoc-amino acids were purchased from AnaSpec (San Jose, CA, USA). Chemicals for the peptide synthesis were obtained from Perkin-Elmer (Foster, CA, USA). Acetonitrile and methanol for HPLC were the products of Burdict and Jackson (Muskegon, MI, USA).

4.2. Peptides synthesis

Peptides were synthesized using standard Fmoc methodology on an automated Applied Biosystem Peptide Synthesizer (Model 433A, Perkin-Elmer, Foster, CA, USA).[22] The peptides were cleaved from the resin by mild trifluoroacetic acid (TFA) cleavage.[23] Purification and analysis of the synthetic peptides were done using a reversed-phase high pressure liquid chromatography (RP-HPLC) system (Waters, Milford, MA, USA). Synthetic peptides were analyzed using a Vydac 218TP54 analytical column under the following gradient conditions: solvent A, 0.1% TFA in water, solvent B, 0.1% TFA in acetonitrile; initial condition 95% A, 25 min, final condition 65% A; flow rate, 1 mL/min. The purity of the synthetic peptides after purification using a Vydac 218TP510 semi-preparative C18 column was above 99%. Peptides were identified by an electrospray mass spectrometer (Platform II, Micromass, Manchester, UK) and an Applied Biosystems 491 Peptide Sequencer (Perkin-Elmer, Foster, CA, USA).

4.3. Assay of HMG-CoA reductase activity

The HMG-CoA-dependent oxidation of NADPH was monitored at 340 nm in a Jasco V-530 spectrophotometer (Model TUDC 1284, Japan Serco Co., Ltd, Japan). Assay conditions were as described in a previous study.[13] One unit (U) of HMGR was defined as the amount of enzyme that catalyzes the oxidation of 1 μmol of NADPH per min. The catalytic domain of Syrian hamster HMGR of 52 kDa was prepared as described in a previous study.[12] Protein concentration was determined by the method of Bradford.[24]

4.4. Circular dichroism spectroscopy

CD spectra were recorded on a Jasco J-710 (JASCO International Co., Tokyo, Japan) spectropolarimeter fitted with a Peltier temperature controller PTC-343 (JASCO International Co., Tokyo, Japan). A quartz cuvette of 0.1 cm light pathlength was used. The UV CD spectra were collected in a range of 190–250 nm. Each spectrum represents the average of five scans obtained by collecting data at intervals of 1 nm, 50 nm/min, and 50 mdeg of sensitivity and was corrected by subtracting the spectrum of a blank solution. Temperature scans were recorded at a heating rate of 0.5 °C/min using a Peltier thermocouple with a resolution of 0.5 °C and a time constant of 8 s. A Fast Fourier Transform program for noise reduction was applied to thermal scan profiles of CD spectra. Secondary structure content was determined by analysis of CD spectra in the 200–240 nm spectral range using a neural net analysis program developed by Andrare et al. (K2D).[25]

4.5. Computational methods

The structures of the peptides and statins were constructed using the program package ChemOffice Desktop 2004 for Windows (CambrigeSoft (CS) Corporation, MA, USA). Calculations of the conformations were carried out using the AM1 method within the CS MOPAC (Version 1.11) program package.[26] The calculations for quantum-chemical optimization were performed using a geometry optimization criterion of 0.001 kcal/mol.

MD simulation was performed using ChemOffice Desktop 2004 for Windows.[27] The peptide structures were collected during 20 ns and heated to 300 K and snapshots from the trajectories were saved every 0.5 ps. The root mean square distance (RMSD) was calculated using the Cartesian coordinate for each model structure of peptides.

The design parameters 'Pr' and 'V' for unconstrained and constrained peptides, respectively, were calculated as described in previous studies.[13,14]

Acknowledgments

This work was supported in part by Project of Functional Food and Development (2006) from the Korea Science and Engineering Foundation (KOSEF) under Ministry of Science and Technology in Korea.
V. V. Pak is a visiting scientist from the Institute of the Chemistry of Plant Substances, Uzbekistan.

References and notes

1. Eisenberg, D. A. *Am. J. Med.* **1998**, *104*, 2S.
2. Hebert, P. R.; Gaziano, J. M.; Chan, K. S.; Hennekens, C. H. *J. Am. Med. Assoc.* **1997**, *278*, 313.
3. Lucer, G.; Lin, B.; Allshouse, J.; Kantor, L. S. *Economic Research Service/USDA* **2000**, *VGS-280*, 458.
4. Kahlon, T. S.; Woodruff, C. L. *Food Chem.* **2002**, *79*, 425.
5. Iwami, K.; Sakakibara, K.; Ibuki, F. *Agric. Biol. Chem.* **1986**, *50*, 1217.
6. Morita, T.; Oh-hashi, A.; Takei, K.; Ikai, M.; Kasaoka, S.; Kiriyama, S. *J. Nutr.* **1997**, *127*, 470.
7. Nagata, Y.; Tanaka, K.; Sugano, M. *J. Nutr. Sci. Vitaminol.* **1981**, *27*, 583.

8. Kim, K. S.; Kim, M. J.; Park, J. S.; Sohn, H. S.; Kwon, D. Y. *Food Sci. Biotechnol.* **2003**, *12*, 153.
9. Kwon, D. Y.; Oh, S. W.; Lee, J. S.; Yang, H. J.; Lee, S. H.; Lee, J. H.; Lee, Y. B.; Sohn, H. S. *Food Sci. Biotechnol.* **2002**, *11*, 55.
10. Pak, V. V.; Koo, M.; Lee, N.; Lee, J. S.; Kasimova, T. D.; Kwon, D. Y. *Chem. Nat. Comp.* **2005**, *41*, 710.
11. Pak, V. V.; Koo, M.; Lee, N.; Lee, J. S.; Kasimova, T. D.; Kwon, D. Y. *Chem. Nat. Comp.* **2005**, *41*, 454.
12. Pak, V. V.; Koo, M.; Lee, N.; Oh, S. K.; Kim, M. S.; Lee, J. S.; Kwon, D. Y. *Food Sci. Biotechnol.* **2005**, *14*, 727.
13. Pak, V. V.; Kim, S. H.; Koo, M.; Lee, N.; Shakhidoyatov, K. M.; Kwon, D. Y. *Biopolymers (Pept. Sci.)* **2006**, *84*, 586.
14. Pak, V. V.; Koo, M.; Yun, L. M.; Kwon, D. Y. *J. Mol. Recogn.* **2007**, *20*, 197.
15. Istvan, E. S.; Palnitkar, M.; Buchanan, K.; Deisenhofer, J. *EMBO J.* **2000**, *19*, 819.
16. Heller, R. A.; Gould, R. G. *J. Biol. Chem.* **1974**, *249*, 5254.
17. Mayer, R. J.; Debouck, C.; Metcalf, B. W. *Arch. Biochem. Biophys.* **1988**, *267*, 110.
18. Luskey, K. L.; Stevens, B. *J. Biol. Chem.* **1985**, *260*, 10271.
19. Chou, T. C.; Talalay, P. *Adv. Enzyme Regul.* **1984**, *22*, 27.
20. Bochar, D. A.; Stauffacher, C. V.; Rodwell, V. W. *Biochemistry* **1999**, *38*, 15848.
21. Istvan, E. S.; Deisenhofer, J. *Science* **2001**, *292*, 1160.
22. Caprino, L. A.; Han, G. Y. *J. Org. Chem.* **1972**, *37*, 3404.
23. Perkin-Elmer Cooperation. *Introduction to Cleavage Techniques*. Perkin-Elmer Cooperation: Foster City, 1995; pp 9–17.
24. Bradford, M. M. *Anal. Biochem.* **1976**, *72*, 248.
25. Andrade, M. A.; Chacón, P.; Merelo, J. J.; Morán, F. *Protein Eng.* **1993**, *6*, 383.
26. Dewar, M. J. S.; Zoebish, E. G.; Healy, E. F.; Stewart, J. J. P. *J. Am. Chem. Soc.* **1985**, *107*, 3902.
27. Kollman, P. A. *Acc. Chem. Res.* **1996**, *29*, 461.